PIBB 生物化学与生物物理进展
Progress in Biochemistry and Biophysics
2024, 51(7): 1687~1696
www.pibb.ac.cn

Hsa-miR-650 Inhibits *NF2*-negative Meningioma Growth by Targeting RAC1*

ZHANG Chao[1,2], LI Peng[1], WANG Bo[1], WANG Ying[1,2]**, LIU Pi-Nan[1,2]**

([1]*Department of Neurosurgery, Beijing Tiantan Hospital, Capital Medical University, Beijing* 100070, China;
[2]*Beijing Neurosurgical Institute, Capital Medical University, Beijing* 100070, China)

Abstract **Objective** This study aimed to identify a potential miRNA-mRNA axis in neurofibromatosis type 2 (*NF2*)-negative meningiomas, investigate their target relationships, and determine their biological functions. **Methods** The GSE17792 dataset, which contains data related to *NF2*-negative meningiomas, was downloaded from the Gene Expression Omnibus (GEO) database. The limma package of R software was used to determine the differentially expressed miRNAs (DeMiRNAs). The miRWalk 2.0 database was applied to obtain the target genes of DeMiRNAs. The Search Tool for the Retrieval of Interacting Genes (STRING) database was utilized to build protein-protein interaction (PPI) networks, and hub genes were identified *via* Cytoscape software. The expression and biological roles of the screened miRNAs were further validated. **Results** Altogether, 86 DeMiRNAs, consisting of 52 upregulated and 34 downregulated miRNAs, were found in *NF2*-negative meningioma tumor samples compared with arachnoid tissue controls. Fourteen miRNAs associated with 274 target genes were identified among these DeMiRNAs, and miRNA-target gene networks were constructed based on these data. Analysis with cytoHubba showed that two miRNAs (hsa-miR-650 and hsa-miR-623) were among the top 20 key hub genes in the PPI network. Further qRT-PCR experimental verification suggested that the expression of hsa-miR-650 was significantly higher in *NF2*-negative meningiomas than in normal brain tissues. Downregulation of hsa-miR-650 inhibited the proliferation and induced the apoptosis of *NF2*-negative meningioma cells. Finally, RAC1 was identified as a target of hsa-miR-650. **Conclusion** Hsa-miR-650 acts as a tumor promoter and might function as a therapeutic target for patients with *NF2*-negative meningiomas.

Key words neurofibromatosis type 2 (NF2), meningiomas, hsa-miR-650, RAC1, bioinformatics
DOI: 10.16476/j.pibb.2023.0349

Neurofibromatosis type 2 (NF2) is a rare, autosomal dominant, multiple neoplasia syndrome that occurs due to mutations in the *NF2* tumor suppressor gene[1-3]. Mutations in *NF2* result in the formation of a series of benign tumors, and meningiomas are considered to be a key factor that affects the severity and progression of this disease[4-5]. Meningiomas caused by *NF2* gene mutations are associated with high morbidity and mortality rates[6-7]. These tumors cannot be cured by surgery alone, and currently available cancer chemotherapeutic agents and radiosurgery are not always effective[8-9]. Therefore, it is important to study the molecular mechanisms of these tumors to develop effective therapeutic drugs.

* This work was supported by grants from The National Natural Science Foundation of China (81974387, 82003023, 82373451), Beijing Municipal Natural Science Foundation (L222015), and Public Welfare Development and Reform Pilot Project of Beijing Medical Research Institute (JYY 2023-2).

** Corresponding author.
LIU Pi-Nan. Tel: 86-10-59976865, Email: pinanliu@ccmu.edu.cn
WANG Ying. Tel: 86-10-59976865, Email: yingwang@ccmu.edu.cn

Received: September 4, 2023 Accepted: January 11, 2024

microRNAs (miRNAs) are small endogenous noncoding RNAs with a total length of 18−25 nucleotides[10-11]. As regulators of negative regulatory genes, miRNAs regulate gene expression at the posttranscriptional level through complete or incomplete complementary to the 3' untranslated regions (3'-UTRs) of their target genes. miRNA dysregulation is commonly observed in diverse tumors, and specific miRNAs participate in various processes in tumors, so the dysregulation of miRNAs is related to tumor progression, apoptosis, and metastasis[12-14]. To date, several studies have shown that miRNAs may be involved in the progression of *NF2*-associated meningiomas[15-16], but the molecular mechanism remains elusive.

In the present study, the miRNA expression profiles of *NF2*-negative meningiomas and arachnoid tissues as a control were downloaded from the National Center for Biotechnology Information (NCBI) Gene Expression Omnibus (GEO) database. Differentially expressed miRNAs (DeMiRNAs) between the two groups were screened, and their target mRNAs were predicted, after which a network consisting of the miRNAs and relevant target genes was built. In addition, a protein-protein interaction (PPI) network was constructed, and finally, the expression of the screened miRNAs in *NF2*-negative meningiomas was validated. The effects of the screened miRNAs on cell proliferation and apoptosis in *NF2*-negative meningiomas was studied *in vitro*, and the underlying molecular mechanisms were explored. Therefore, this study reveals a potential regulatory mechanism and provides valuable insights for further functional study of *NF2*-negative meningiomas.

1 Materials and methods

1.1 Data collection

The dataset GSE17792[16] (https://www.ncbi.nlm.nih.gov/geo/query/acc.cgi?acc=GSE17792) was downloaded from the GEO database. In total, 7 *NF2*-negative meningioma tumor samples and 3 arachnoid tissue control samples were included in this study, and two technical replicates were performed for each sample.

1.2 Differential expression analysis

The initial CEL data underwent transformation using the oligo package (Version 1.34.2) in R software (Version 3.5.2), followed by preprocessing utilizing the robust multiarray average (RMA) algorithm. The Benjamini and Hochberg method was used to perform multiple test corrections of the *P* value. The parameters used to screen differential expression were set as a $P<0.05$ and $|\log_2 FC|>1$. In addition, a volcano plot was made using the ggplot2 package[17] in R to determine the DeMiRNAs whose expression was statistically different between the two groups.

1.3 miRNA–target gene network construction

Based on the above analysis, DeMiRNAs from the 7 cases of *NF2*-negative meningiomas and 3 cases arachnoid tissue were isolated, and the DeMiRNAs were used to predict potential target genes. Furthermore, the miRDB[18] (https://mirdb.org/) and TargetScan[19] (https://www.targetscan.org/vert_80/) databases were also used to predict potential target genes. The DeMiRNAs were screened, and a miRNA-target gene network was constructed by using Cytoscape (3.7.2)[20] (https://cytoscape.org/).

1.4 PPI regulatory network analysis

We used the STRING database (version 11.0)[21] (https://cn.string-db.org/) to construct a PPI network to show the relationships of the DeMiRNAs. A comprehensive score over 0.9 was used to indicate statistical significance, and we hid nodes that were not connected with other entities in the network. Cytoscape (version 3.7.2) was used to construct the network, and the hub genes in the PPI network were analyzed using cytoHubba in Cytoscape (version 3.7.2)[20].

1.5 Samples

Thirty meningioma tumor tissue samples and 3 normal brain tissue samples were surgically resected from meningioma patients at Beijing Tiantan Hospital. The work described was carried out in accordance with The Code of Ethics of the World Medical Association. Our study protocols were approved by the Institutional Review Board of Beijing Tiantan Hospital (KY2019-135-01), and written

informed consent was obtained from the patients prior to their participation.

1.6 Cell culture and CCK8 assay

Briefly, three shRNA that target *NF2* were designed to maximize interference. The shRNA (GV493-NF2 shRNA) and negative control were synthesized at Genechem. The IOMM-Lee cells were transfected with GV493-NF2 shRNA, after 72 h, the transfected cells were selected with puromycin. The IOMM-LeeNF2-KD cells, which were obtained by screening for puromycin resistance to achieve stable knockdown of *NF2* gene, were utilized for subsequent experimental investigations. Meningioma cells (IOMM-Lee$^{NF2\text{-}KD}$ cells) were cultured in 10% FBS-containing DMEM and maintained in a humidified atmosphere containing 5% CO_2 at 37℃. The viability of the IOMM-Lee$^{NF2\text{-}KD}$ cells was measured with a CCK8 assay (Dojindo, Kumamoto, Japan). After transfection with an hsa-miR-650 inhibitor for 48 h, the cells (1×10^4/well) were cultured in 96-well plates overnight, a 10% CCK8 solution was added to each well, and the cells were incubated at 37℃ for 2 h. Subsequently, the absorption was detected using a SpectraMax M5 instrument (Molecular Devices, Sunnyvale, CA, U.S.A.) at 450 nm.

1.7 Apoptosis analysis

Apoptosis was measured using an apoptosis detection kit (BD, CA, USA). After 72 h of transfection with the hsa-miR-650 inhibitor, the fluorescence intensities of the IOMM-Lee$^{NF2\text{-}KD}$ cells were determined by flow cytometry (BD, CA, USA).

1.8 Quantitative reverse transcription polymerase chain reaction （qRT−PCR）

The primers were purchased from RiboBio (Guangzhou, China), the detailed information is as follows.

MiR-650, F: miDETECT A Track hsa-miR-650 Forward Primer (miRA1000043-1-100, RIBOBIO), R: Universal reverse primer miDETECT A TrackTM Uni-Reverse Primer.

U6, F: miDETECT A Track U6 Forward Primer (miRAN0002-1-200, RIBOBIO), R: Universal reverse primer miDETECT A TrackTM Uni-Reverse Primer.

Reverse Transcription and RT-PCR were performed using miDETECT A Track miRNA qRT-PCR Starter Kit (C10712-2, RIBOBIO).

1.9 Western blot

Total proteins from different treated cells were extracted using radio immunoprecipitation assay lysis buffer (RIPA, PPLYGEN). After measuring the protein concentration, 20−40 μg of protein per sample was separated by 12% SDS-polyacrylamide gel electrophoresis (SDS-PAGE) and then transferred to polyvinylidene difluoride membranes (PALL, USA). The membranes were then blocked at room temperature for 2 h with 5% nonfat milk and incubated at 4℃ overnight with primary detection antibodies, followed by incubation with the appropriate HRP-conjugated secondary antibody and detection by a Western-Light Chemiluminescent Detection System (Millipore, USA). ImageJ software (NIH, USA) was used to analyze the relative density of immunoreactive bands.

2 Results

2.1 Identification of DeMiRNAs

A total of 409 miRNAs were screened after data preprocessing. Among these miRNAs, 86 DeMiRNAs were identified, including 52 upregulated miRNAs (60.47%) (Table S1) and 34 downregulated miRNAs (39.53%). Volcano plots were generated to show the distribution of the DeMiRNAs, and the top 20 down-regulated and top 20 up-regulated DeMiRNAs are listed in Figure 1.

2.2 miRNA−target gene network construction

The construction of the miRNA-target regulatory network is of significant importance in elucidating cellular regulatory networks, discovering new target genes, identifying miRNA functions and disease relevance, as well as facilitating drug development. Genes targeted by the miRNAs were predicted using the miRDB and TargetScan databases. A total of 14 miRNAs (6 upregulated miRNAs and 8 downregulated miRNAs) with the number of target

(a)

miRNA_ID	log_2FC	*P*
hsa-miR-19b-1	−8.297 93	0.001 18
hsa-miR-125a	−8.260 40	0.000 18
hsa-miR-17-5p	−7.728 01	0.000 16
hsa-let-7d	−7.198 21	0.002 10
hsa-miR-335	−7.136 01	0.000 16
hsa-miR-551b	−7.059 25	0.016 66
hsa-let-7g	−7.051 68	0.000 48
hsa-miR-221	−6.967 09	0.000 77
hsa-miR-125b-5p	−6.368 39	0.001 94
hsa-miR-376b	−6.329 37	0.005 98
hsa-miR-27a	−6.264 61	0.000 18
hsa-miR-299	−6.204 01	0.002 65
hsa-miR-146	−5.648 77	0.005 13
hsa-miR-151	−5.616 81	0.002 40
hsa-miR-106a	−5.522 29	0.016 96
hsa-miR-139	−5.075 04	0.008 58
hsa-miR-106b	−5.059 89	0.002 66
hsa-miR-34a	−4.989 51	0.005 38
hsa-miR-21	−4.822 96	0.026 55
hsa-let-7i	−4.741 49	0.030 53

(b)

miRNA_ID	log_2FC	*P*
hsa-miR-28	7.056 47	0.002 46
hsa-miR-524	6.726 22	0.005 23
hsa-miR-518a-2	6.679 10	0.005 26
hsa-miR-93	6.487 67	0.007 53
hsa-miR-NC18-3	6.249 20	0.015 92
hsa-miR-433-3p	5.947 86	0.013 20
hsa-miR-516-5p	5.775 31	0.031 61
hsa-miR-138	5.574 73	0.022 79
hsa-miR-NC16-1	5.553 65	0.027 38
hsa-miR-521	5.520 04	0.012 71
hsa-miR-302a	5.392 93	0.028 01
hsa-miR-518f	5.259 54	0.035 57
hsa-miR-422a	5.177 03	0.018 11
hsa-miR-34b	5.166 68	0.021 29
hsa-miR-496	5.148 46	0.048 99
hsa-miR-432	4.982 10	0.036 07
hsa-miR-485-5p	4.964 33	0.010 66
hsa-miR-298	4.957 89	0.040 23
hsa-miR-351	4.860 85	0.009 61
hsa-miR-510	4.853 46	0.027 33

(c)

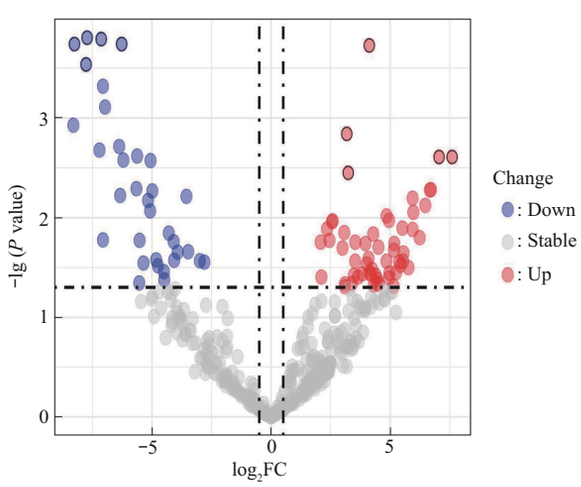

Fig. 1 Differentially expressed miRNAs (DeMiRNAs)

(a) Top 20 down-regulated miRNAs. (b) Top 20 up-regulated miRNAs. (c) Volcano plot of DeMiRNAs. Upregulated genes are marked in red; downregulated genes are marked in blue. DeMiRNAs were selected with the thresholds fold change>2 and $P<0.05$.

genes≥5 was identified. The upregulated miRNAs included hsa-miR-298, hsa-miR-650, hsa-miR-608, hsa-miR-492, hsa-miR-206 and hsa-miR-623. Additionally, the above mentioned 274 target genes consisted of 86 target genes that interact with the upregulated miRNAs and 195 target genes that interact with the downregulated miRNAs. Subsequently, an upregulated miRNA-target gene (target genes≥5) regulatory network was constructed (Figure 2). By constructing a miRNA-target regulatory network, we have identified new miRNA target genes, thereby assisting us to understand the gene regulatory network in further.

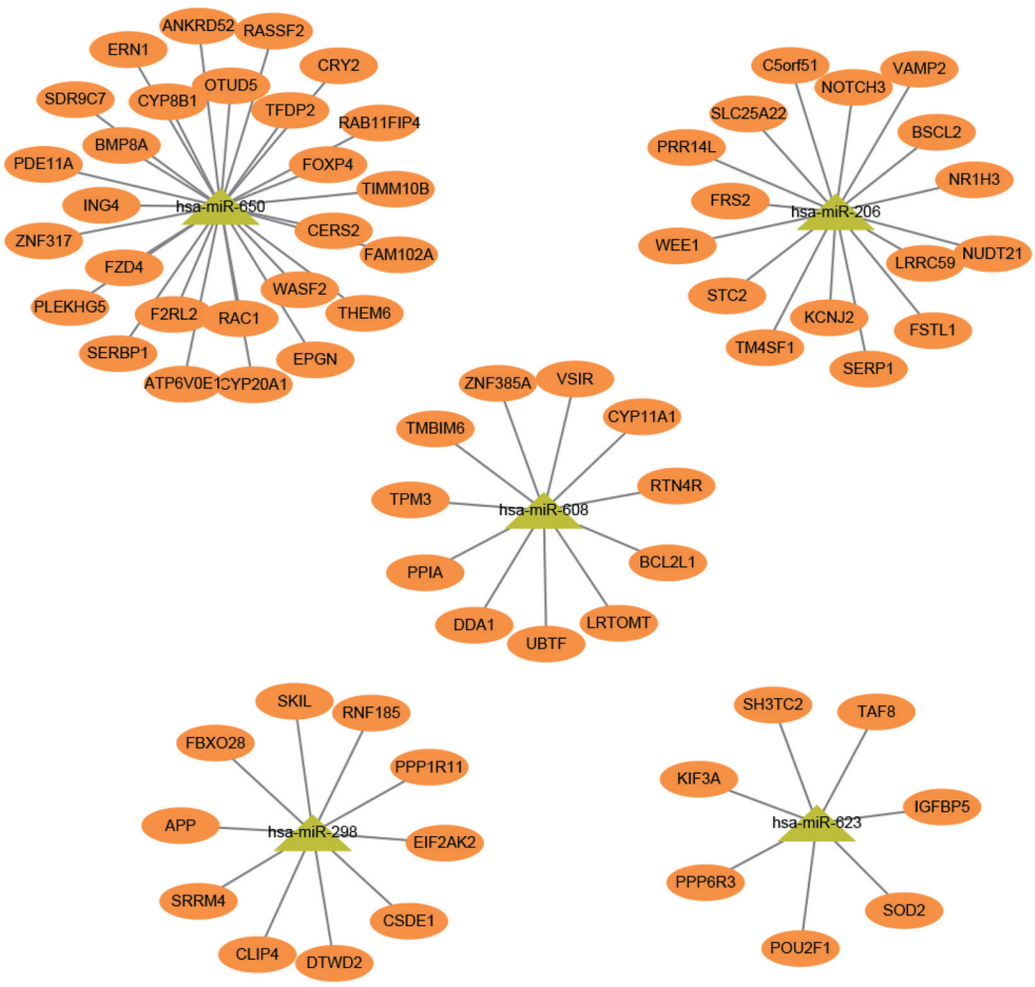

Fig. 2 Interaction network consisting of upregulated DeMiRNAs and related target genes

Yellow nodes: upregulated DeMiRNAs; orange nodes: target genes.

2.3 Construction of a PPI network

PPI analysis plays a crucial role in understanding cellular processes, identifying protein functions, discovering therapeutic targets, and predicting protein structures and functions. It serves as a valuable tool in systems biology, drug discovery, and functional genomics research. The STRING online database (version 11.3) and Cytoscape software (version 3.7.2) were used to explore the PPI network, with score of >0.9. The network consisted of 94 nodes and 164 protein pairs (Figure 3).

Moreover, the top 20 key hub nodes (APP, hsa-miR-650, IGFBP5, CCND2, FSTL1, STC2, hsa-miR-206, NOTCH3, BCL2L1, hsa-miR-623, Ras-related C3 botulinum toxin substrate 1 (RAC1), VAMP2, AGO2, BCL6, ERN1, ANKRD52, SOD2, TMBIM6, POU2F1, and WEE1) ranked by the MCC method were analyzed (Figure 4). By mapping and analyzing disease-related PPI networks, we can help identify key proteins or protein complexes in *NF2*-negative meningiomas that could serve as therapeutic targets, thereby contributing to the development of novel drugs and therapies.

2.4 Hsa−miR−650 is upregulated in *NF2*−negative meningiomas

Next, we validated the relative expression levels of hsa-miR-650 and hsa-miR-623 in 30 *NF2*-negative meningiomas and 3 normal brain tissue samples as controls using qRT-PCR. The results showed that the relative hsa-miR-650 expression level was significantly higher than that in the normal brain tissue control samples (Figure 5a).

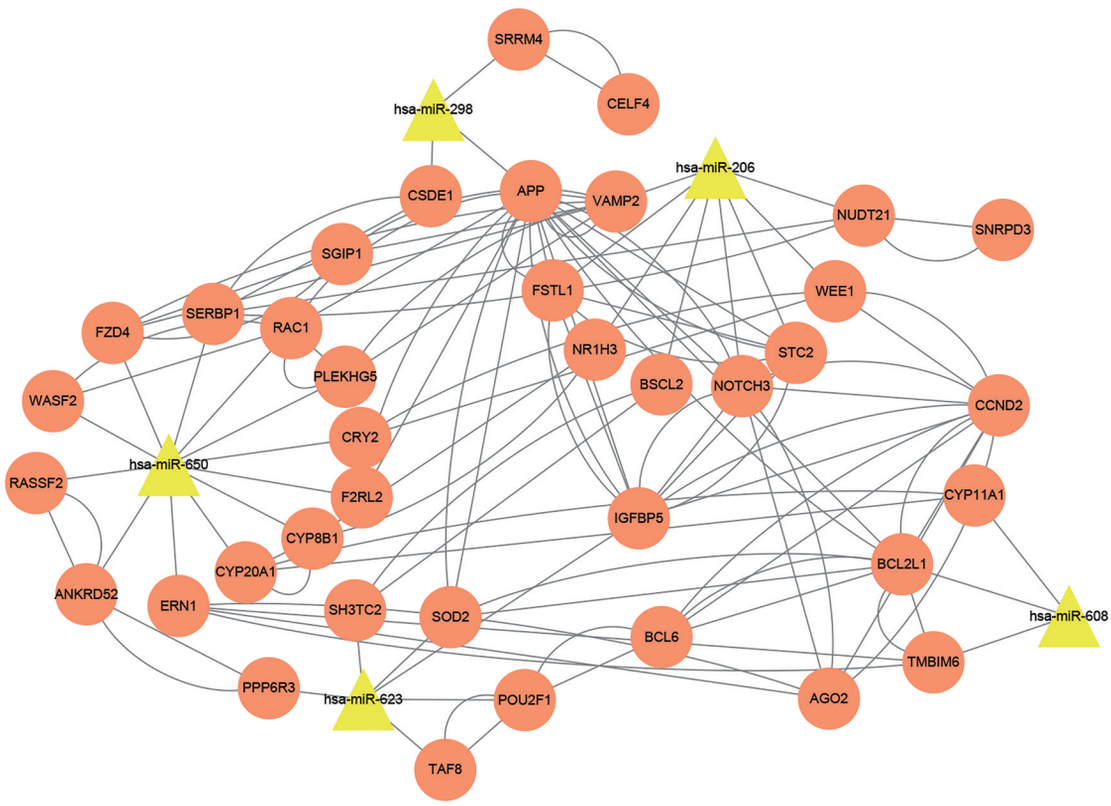

Fig. 3　Protein−protein interaction（PPI）network of upregulated miRNAs constructed using STRING software

Yellow nodes: upregulated DeMiRNAs; orange nodes: target genes.

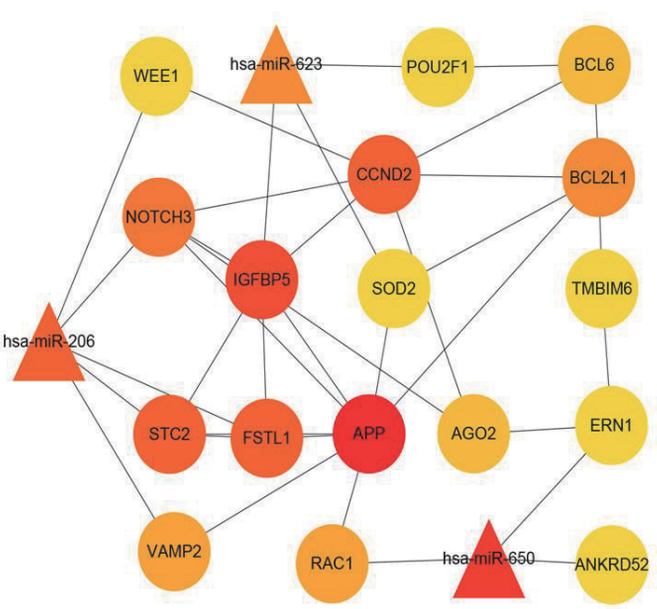

Top 20 in network ranked by MCC method

Rank	Name	Score
1	APP	14
2	hsa-miR-650	13
3	IGFBP5	11
4	CCND2	8
4	FSTL1	8
4	STC2	8
4	hsa-miR-206	8
8	NOTCH3	7
9	BCL2L1	6
9	hsa-miR-623	6
11	RAC1	5
11	VAMP2	5
13	AGO2	4
13	BCL6	4
15	ERN1	3
15	ANKRD52	3
15	SOD2	3
15	TMBIM6	3
15	POU2F1	3
15	WEE1	3

Fig. 4　Top 20 hub nodes ranked by the MCC method in the PPI network

Triangle nodes: upregulated DeMiRNAs; circle nodes: target genes.

2.5 Downregulation of hsa−miR−650 inhibits the proliferation of *NF2*−deficient meningioma cells

To characterize the role of hsa-miR-650 in *NF2*-deficient meningioma, a stable *NF2*-knockdown IOMM-Lee cell line (IOMM-Lee$^{NF2\text{-}KD}$) was established at first (Figure S1), and then the IOMM-Lee$^{NF2\text{-}KD}$ cells were selected for transfection with an hsa-miR-650 inhibitor (micrOFF hsa-miR-650 inhibitor (miR20003320-1-5)) to knock down endogenous hsa-miR-650 expression. Next, CCK8 and apoptosis assays were performed to determine the potential effects of hsa-miR-650 in *NF2*-deficient meningiomas. The results showed that the knockdown of hsa-miR-650 significantly inhibited cell proliferation (Figure S2) and increased apoptosis. Further Western blot results showed that expression of the apoptosis-related proteins Cleaved-caspase3 and Bax was increased while the expression of Bcl-2 was decreased (Figure 5b−d).

2.6 Hsa−miR−650 activates RAC1 in *NF2*−deficient meningiomas

RAC1 was predicted to be a target of hsa-miR-650 through bioinformatic analysis. To validate whether hsa-miR-650 inhibits *NF2*-negative meningioma cell proliferation by targeting RAC1, we constructed IOMM-Lee$^{NF2\text{-}KD}$ cells with increased and decreased hsa-miR-650 and RAC1 expression. The inhibitory effect of hsa-miR-650 suppression on cell proliferation was restored by RAC1 overexpression. The ability of hsa-miR-650 upregulation to promote cell proliferation was attenuated by RAC1 suppression. Western blot results showed that the inhibitory effect of hsa-miR-650 on RAC1 expression could be restored by RAC1 transfection (Figure 5e, f).

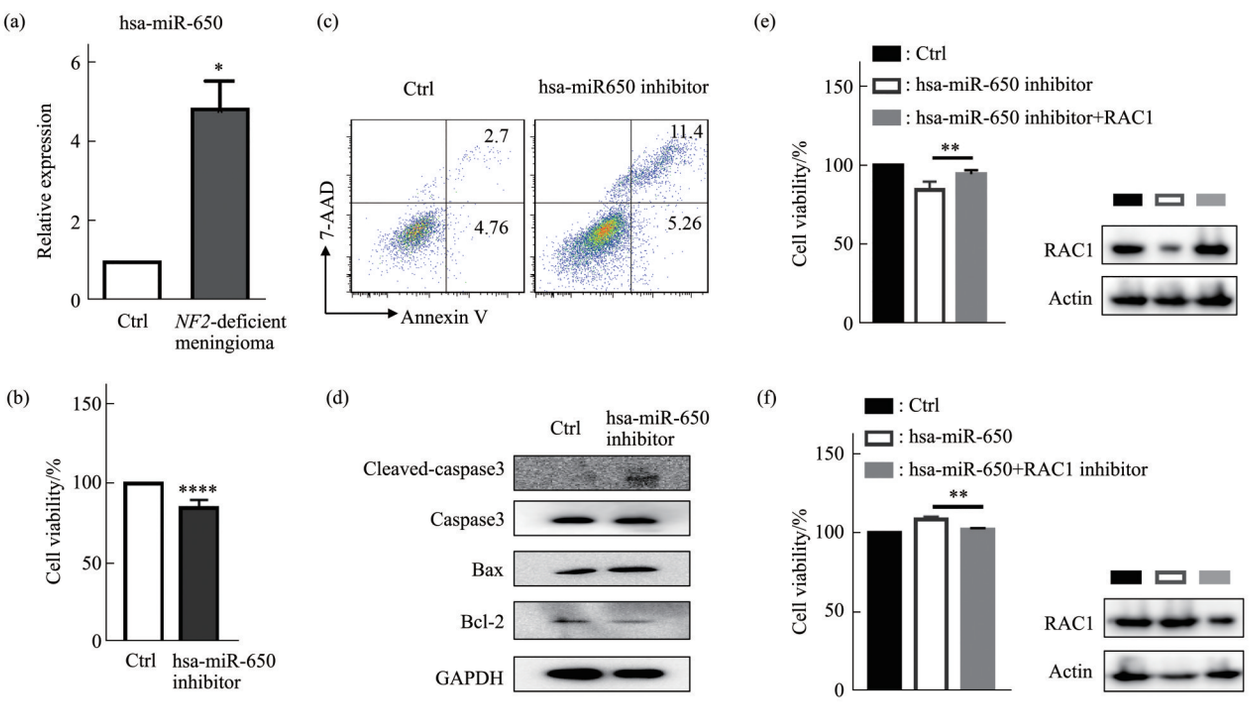

Fig. 5 Hsa−miR−650 inhibits the proliferation of *NF2*−negative meningioma cells by targeting RAC1

(a) Hsa-miR-650 is more highly expressed in *NF2*-negative meningioma tissues (n=30) than in normal brain tissues (n=3). (b−d) Knockdown of hsa-miR-650 inhibited cell proliferation and induced apoptosis. (e) The inhibitory effect of hsa-miR-650 suppression on cell proliferation could be restored by RAC1 overexpression. (f) The ability of hsa-miR-650 upregulation to promote cell proliferation was attenuated by RAC1 suppression. **P*<0.05, ***P*<0.01, *****P*<0.000 1.

3 Discussion

In this study, we performed a comprehensive analysis to screen DeMiRNAs between *NF2*-negative meningiomas and arachnoid tissue controls. We identified 14 DeMiRNAs that are associated with 274 target genes, including 5 upregulated miRNAs (hsa-miR-298, hsa-miR-650, hsa-miR-608, hsa-miR-206

and hsa-miR-623) associated with ≥5 target genes. The cytoHubba analysis showed that two of the upregulated miRNAs (hsa-miR-650 and hsa-miR-623) were listed among the top 20 key hub genes in the PPI network. Further experimental verification suggested that the expression of hsa-miR-650 was significantly higher in *NF2*-negative meningiomas than in the normal brain tissues as a control group, and the downregulation of hsa-miR-650 inhibited the proliferation and apoptosis of *NF2*-negative meningioma cells by targeting RAC1.

miRNAs play important roles in biological processes such as gene expression regulation, development, metabolism, and immunity. They are crucial for the overall development and health status of cells and organisms. Through biological information analysis, we discovered that hsa-miR-650 and hsa-miR-623 were listed among the top 20 key hub genes in the PPI network. Recent studies have indicated that hsa-miR-650 is involved in various cancers[22-23]. For example, hsa-miR-650 has displayed oncogenic activity in anaplastic thyroid carcinoma cells by targeting PPP2CA phosphatase, suggesting that the miR-650/PPP2CA axis can be modulated to interfere with the motility of thyroid carcinoma cells[24]. Additionally, hsa-miR-650 was found to be upregulated in glioma tissues, to promote cell proliferation, migration and invasion in glioma cells, and to enhance glioma tumor formation and growth *in vivo*[25], revealing novel functional roles for hsa-miR-650 in glioma development and providing new avenues for future clinical applications.

Our further experimental validation results indicate that hsa-miR-650 is significantly upregulated in *NF2*-negative meningiomas. Knockdown of hsa-miR-650 inhibited cell proliferation and promoted cell apoptosis in *NF2*-negative meningioma cells. Additionally, RAC1 was identified as a target of hsa-miR-650.

NF2 (also known as merlin) is a tumor suppressor protein encoded by the *NF2* gene, and studies have proven its involvement in several signaling pathways[26-28]. Previous studies have proven that merlin-mediated contact inhibition is critically regulated by RAC1[29-30]; furthermore, the loss of merlin is related to elevated RAC1 activity in NF2 patients, and RAC1 activity could be inhibited by the overexpression of NF2[31-32]. The above evidence indicates the importance of RAC1 in the occurrence and development of NF2. In this study, we predicted that *RAC1* is a target gene of hsa-miR-650 using bioinformatics tools, and the results of further rescue experiments showed that the gain of RAC1 function partially restored the inhibitory effect of hsa-miR-650 upregulation on cell proliferation, indicating that hsa-miR-650 regulates cell proliferation by regulating RAC1.

In summary, the results of this paper demonstrated that hsa-miR-650 was upregulated in *NF2*-negative meningiomas and that the downregulation of hsa-miR-650 inhibited cell proliferation and induced apoptosis in *NF2*-negative meningioma cells. In addition, RAC1 was identified as a target of hsa-miR-650. These results indicate that hsa-miR-650 acts as a tumor promoter and might function as a therapeutic target for patients with *NF2*-negative meningiomas.

4 Conclusion

In this study, we demonstrated that hsa-miR-650 was significantly higher in *NF2*-negative meningiomas. Downregulation of hsa-miR-650 inhibited the proliferation and induced the apoptosis of *NF2*-negative meningioma cells by regulating RAC1. This study may provide reliable experimental data for new therapeutic target for patients with *NF2*-negative meningiomas.

Supplementary Available online (http://www.pibb.ac.cn or http://www.cnki.net):
PIBB_20230349_Table_S1.pdf
PIBB_20230349_Figure_S1.pdf
PIBB_20230349_Figure_S2.pdf

References

[1] Tamura R. Current understanding of neurofibromatosis type 1, 2, and Schwannomatosis. Int J Mol Sci, 2021, **22**(11): 5850

[2] Halliday D, Parry A, Evans DG. Neurofibromatosis type 2 and related disorders. Curr Opin Oncol, 2019, **31**(6): 562-567

[3] Asthagiri A R, Parry D M, Butman J A, *et al*. Neurofibromatosis type 2. Lancet, 2009, **373**(9679): 1974-1986

[4] Bachir S, Shah S, Shapiro S, *et al*. Neurofibromatosis type 2 (NF2) and the implications for vestibular Schwannoma and meningioma pathogenesis. Int J Mol Sci, 2021, **22**(2): 690

[5] Baser M E, Friedman J M, Aeschliman D, *et al*. Predictors of the risk of mortality in neurofibromatosis 2. Am J Hum Genet, 2002, **71**(4): 715-723

[6] Dirks M S, Butman J A, Kim H J, *et al*. Long-term natural history

of neurofibromatosis type 2-associated intracranial tumors. J Neurosurg, 2012, **117**(1): 109-117

[7] Birzu C, Peyre M, Sahm F. Molecular alterations in meningioma: prognostic and therapeutic perspectives. Curr Opin Oncol, 2020, **32**(6): 613-622

[8] Karajannis M A, Ferner R E. Neurofibromatosis-related tumors: emerging biology and therapies. Curr Opin Pediatr, 2015, **27**(1): 26-33

[9] Voizard B, Maniakas A, Saliba I. Office-based stapes surgery. Otolaryngol Head Neck Surg, 2019, **161**(6): 1018-1026

[10] Bhaskaran M, Mohan M. MicroRNAs: history, biogenesis, and their evolving role in animal development and disease. Vet Pathol, 2014, **51**(4): 759-74

[11] Saliminejad K, Khorram Khorshid H R, Soleymani Fard S, *et al*. An overview of microRNAs: Biology, functions, therapeutics, and analysis methods. J Cell Physiol, 2019, **234**(5): 5451-5465

[12] Lee Y S, Dutta A. MicroRNAs in cancer. Annu Rev Pathol, 2009, **4**: 199-227

[13] Hayes J, Peruzzi P P, Lawler S. MicroRNAs in cancer: biomarkers, functions and therapy. Trends Mol Med, 2014, **20**(8):460-469

[14] Cowland J B, Hother C, Grønbaek K. MicroRNAs and cancer. APMIS, 2007, **115**(10): 1090-106

[15] Galani V, Lampri E, Varouktsi A, *et al*. Genetic and epigenetic alterations in meningiomas. Clin Neurol Neurosurg, 2017, **158**: 119-125

[16] Saydam O, Shen Y, Würdinger T, *et al*. Downregulated microRNA-200a in meningiomas promotes tumor growth by reducing E-cadherin and activating the Wnt/beta-catenin signaling pathway. Mol Cell Biol, 2009, **29**(21): 5923-5940

[17] Ito K, Murphy D. Application of ggplot2 to pharmacometric graphics. CPT Pharmacometrics Syst Pharmacol, 2013, **2**(10): e79

[18] Chen Y, Wang X. miRDB: an online database for prediction of functional microRNA targets. Nucleic Acids Res, 2020, **48**(D1): D127-D131

[19] Mon-López D, Tejero-González CM. Validity and reliability of the TargetScan ISSF Pistol & Rifle application for measuring shooting performance. Scand J Med Sci Sports, 2019, **29**(11): 1707-1712

[20] Shannon P, Markiel A, Ozier O, *et al*. Cytoscape: a software environment for integrated models of biomolecular interaction networks. Genome Res, 2003, **13**(11): 2498-504

[21] Szklarczyk D, Franceschini A, Kuhn M, *et al*. The STRING database in 2011: functional interaction networks of proteins, globally integrated and scored. Nucleic Acids Res, 2011, **39**(Database issue): D561-D568

[22] Xu L, Yu Q W, Fang S Q, *et al*. MiR-650 inhibits the progression of glioma by targeting FAM83F. Eur Rev Med Pharmacol Sci, 2018, **22**(23): 8391-8398

[23] Zhou C, Cui F, Li J, *et al*. MiR-650 represses high-risk non-metastatic colorectal cancer progression *via* inhibition of AKT2/GSK3β/E-cadherin pathway. Oncotarget, 2017, **8**(30): 49534-49547

[24] Orlandella F M, Mariniello R M, Iervolino P, *et al*. miR-650 promotes motility of anaplastic thyroid cancer cells by targeting PPP2CA. Endocrine, 2019, **65**(3): 582-594

[25] Jin S, Li X, Dai Y, *et al*. NF-κB-mediated miR-650 plays oncogenic roles and activates AKT/ERK/NF-κB pathways by targeting RERG in glioma cells. Cell Oncol (Dordr), 2020, **43**(6): 1035-1048

[26] Petrilli A M, Fernández-Valle C. Role of Merlin/NF2 inactivation in tumor biology. Oncogene, 2016, **35**(5): 537-548

[27] Schulz A, Zoch A, Morrison H. A neuronal function of the tumor suppressor protein merlin. Acta Neuropathol Commun, 2014, **2**: 82

[28] Morrow K A, Shevde L A. Merlin: the wizard requires protein stability to function as a tumor suppressor. Biochim Biophys Acta, 2012, **1826**(2): 400-406

[29] Guo L, Moon C, Niehaus K, *et al*. Rac1 controls Schwann cell myelination through cAMP and NF2/merlin. J Neurosci, 2012, **32**(48): 17251-17261

[30] Manchanda P K, Jones G N, Lee A A, *et al*. Rac1 is required for Prkar1a-mediated Nf2 suppression in Schwann cell tumors. Oncogene, 2013, **32**(30): 3491-3499

[31] Zhou L, Ercolano E, Ammoun S, *et al*. Merlin-deficient human tumors show loss of contact inhibition and activation of Wnt/β-catenin signaling linked to the PDGFR/Src and Rac/PAK pathways. Neoplasia, 2011, **13**(12): 1101-1112

[32] Wong H K, Shimizu A, Kirkpatrick N D, *et al*. Merlin/NF2 regulates angiogenesis in Schwannomas through a Rac1/semaphorin 3F-dependent mechanism. Neoplasia, 2012, **14**(2): 84-94

Hsa-miR-650通过靶向RAC1抑制*NF2*阴性脑膜瘤的生长*

张 超[1,2] 李 朋[1] 王 博[1] 汪 颖[1,2]** 刘丕楠[1,2]**

（[1] 首都医科大学附属北京天坛医院神经外科，北京 100070；
[2] 首都医科大学，北京市神经外科研究所，北京 100070）

摘要 **目的** 本文旨在确定*NF2*表达阴性脑膜瘤中潜在的miRNA-mRNA轴，研究它们的靶向关系，并确定它们的生物学功能。**方法** 从基因表达数据库（GEO）下载包含与*NF2*阴性脑膜瘤相关数据的GSE17792数据集。使用R软件中的limma包确定差异表达的miRNA（DeMiRNAs）。应用miRWalk 2.0数据库获取DeMiRNAs的靶基因。利用相互作用基因检索工具（STRING）数据库构建蛋白质相互作用（PPI）网络，并通过Cytoscape软件确定核心基因。对筛选出的miRNA进一步验证其表达和生物学作用。**结果** 在*NF2*阴性脑膜瘤肿瘤样本与蛛网膜组织对照组比较中发现了86个差异miRNA，其中包括52个上调的miRNAs和34个下调的miRNAs。在这些差异miRNA中鉴定出与274个靶基因相关的14个miRNAs，并基于这些数据构建miRNA-靶基因网络。通过cytoHubba分析显示，在PPI网络中有两个miRNAs（hsa-miR-650和hsa-miR-623）位于前20个关键核心基因之中。进一步的定量逆转录PCR（qRT-PCR）实验证实，相对于正常脑组织，hsa-miR-650在*NF2*阴性脑膜瘤中的表达显著增高。下调hsa-miR-650抑制了*NF2*阴性脑膜瘤细胞的增殖并诱导细胞凋亡。最后，确定*RAC1*是hsa-miR-650的靶基因。**结论** Hsa-miR-650作为肿瘤促进剂，可能作为治疗*NF2*阴性脑膜瘤患者的治疗靶点。

关键词 2型神经纤维瘤病（NF2），脑膜瘤，hsa-miR-650，RAC1，生物信息学
中图分类号 R73 **DOI**：10.16476/j.pibb.2023.0349

* 国家自然科学基金（81974387，82003023，82373451），北京市自然海淀联合基金-海淀原始创新联合基金（L222015）和北京市属医学科研院所公益发展改革试点项目（京医研2023-2）资助。
** 通讯联系人。
刘丕楠 Tel：010-59976865，E-mail：pinanliu@ccmu.edu.cn
汪颖 Tel：010-59976775，E-mail：yingwang@ccmu.edu.cn
收稿日期：2023-09-04，接受日期：2024-01-11